Ion Thruster Modeling: Particle Simulations and Experimental Validations

Article · May 2003

DOI: 10.1063/1.1581590

3 authors:

Joseph Wang
University of Southern California
156 PUBLICATIONS **2,403** CITATIONS
SEE PROFILE

Jay Polk
California Institute of Technology
196 PUBLICATIONS **3,040** CITATIONS
SEE PROFILE

David E Brinza
California Institute of Technology
113 PUBLICATIONS **6,850** CITATIONS
SEE PROFILE

Ion Thruster Modeling: Particle Simulations and Experimental Validations

Joseph Wang*, James Polk† and David Brinza†

*Virginia Polytechnic Institute and State University, Blacksburg, VA 24061, USA
†Jet Propulsion Laboratory, Pasadena, CA 91109, USA

Abstract. This paper presents results from ion thruster modeling studies performed in support of NASA's Deep Space 1 mission and NSTAR project. Fully 3-dimensional computer particle simulation models are presented for ion optics plasma flow and ion thruster plume. Ion optics simulation results are compared with measurements obtained from ground tests of the NSTAR ion thruster. Plume simulation results are compared with in-flight measurements from the Deep Space 1 spacecraft. Both models show excellent agreement with experimental data.

INTRODUCTION

Ion propulsion is a critical enabling technology for future deep space missions. NASA's New Millennium Deep Space 1 (DS1) marks the beginning of interplanetary missions using spacecraft operated with ion propulsion. Using a 30cm diameter xenon ion thruster developed under NASA's NSTAR project as its primary propulsion system, DS1 successfully flew by asteroid Braille in July 28 1999 and comet Borrelly in October 2001. Fig. 1 shows the DS1 spacecraft and the NSTAR ion thruster used on DS1. Currently, ion propulsion is being considered for use on several upcoming NASA missions, and new, high power ion engines are also being developed.

An ion engine propels a spacecraft by continuously emitting a high speed plasma flow over long periods of time. This raises two key questions in ion thruster design and integration with spacecraft. First, how does one design a thruster that has both optimized thruster performance and long service lifetime for a given mission requirement? Second, how does one quantitatively predict the effects from thruster plume on spacecraft and science measurement to ensure that spacecraft reliability and science return would not be compromised? Obviously, these two issues must be fully resolved if ion propulsion is to become a legitimate choice for future space missions.

Due to the complex nature of the physics involved and a lack of flight testing opportunity, physics based modeling is playing an ever more important role in ion thruster research and development activities. As part of the Deep Space 1 mission and the NSTAR project, several modeling studies were carried out to understand ion thruster service life limit and to quantify the effects of ion thruster plume on spacecraft and plasma measurements. This paper presents an overview of the results from two of these modeling studies.

As illustrated in Fig. 2, an ion engine has three main components: discharge chamber, ion optics, and neutralizer. The propellant is ionized in the discharge chamber by electron bombardment. The propellant ions are then accelerated electrostatically by a system of grids to form a high velocity beam to provide thrust. The electrons are emitted from a neutralizer to neutralize the space charge of the ion beam. An ion engine presents a wide spectrum of interesting problems related to plasma flow. One may categorize ion thruster plasma flow into the following four categories: i)plasma flow inside discharge chamber and neutralizer; ii)ion optics plasma flow; iii)near-spacecraft thruster plume; and iv)far-field thruster plume. Thruster service life and grid design issues are primarily determined by physical processes in the ion optics. Plume effects on spacecraft are primarily determined by physical processes near spacecraft. Hence, in this paper, we limit our discussions to ion optics plasma flow and near-spacecraft plume. While those plasma processes inside the discharge chamber and neutralizer and in the region far from spacecraft are also important issues, they will not be addressed in this paper.

Section II provides some background on ion optics and ion thruster plume and briefly discusses the modeling approach. Section III presents 3-dimensional particle simulations of ion optics plasma flow and grid erosion. Simulation results are compared with grid erosion measurements obtained during the long duration test of the NSTAR ion thruster performed at JPL. Section IV presents 3-dimensional particle simulations of ion thruster plume plasma environment. Simulation results are compared with in-flight measurements obtained from the Deep Space 1 spacecraft. Section V contains a summary and conclusions.

CP663, *Rarefied Gas Dynamics: 23rd International Symposium*, edited by A. D. Ketsdever and E. P. Muntz

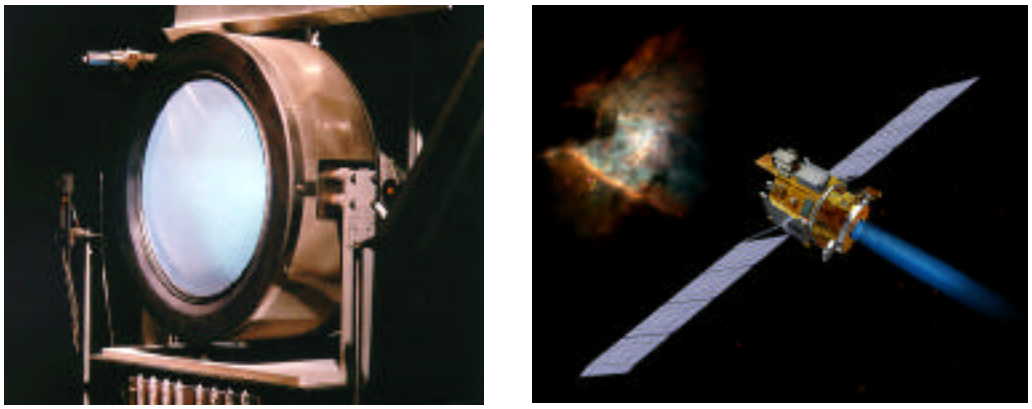

Fig. 1: The NSTAR ion thruster (left) and the Deep Space 1 spacecraft (right) (Courtesy of JPL)

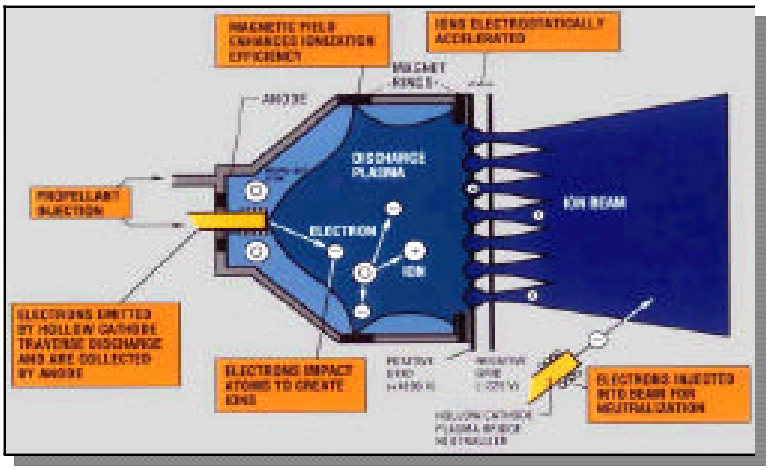

Fig. 2: Illustration of ion thruster operation

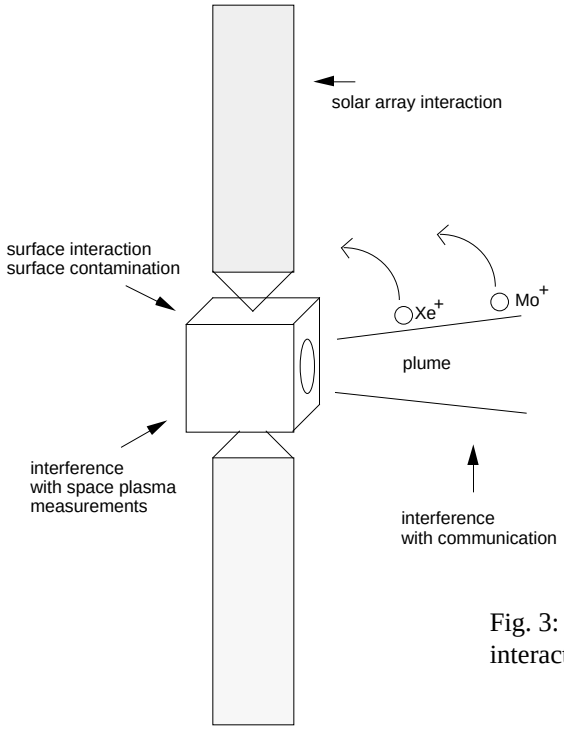

Fig. 3: Illustration of ion thruster plume-spacecraft interactions

TABLE 1. Nominal geometric and operating parameters for the NSTAR ion engine

	hole diameter	grid thickness	grid voltage
screen grid	1.91 mm	0.38 mm	1074 V
accel grid	1.14 mm	0.51 mm	-180 V
	center-to-center hole spacing	screen-to-accel grid gap	total accelerating voltage
	2.21 mm	0.58 mm	1100 V

FORMULATION AND APPROACH

Ion Optics Plasma Flow

The ion optics is the component that accelerates the propellant ions to produce thrust. As shown in Fig. 2, an ion optics is composed of a screen grid and an accelerator grid. The electric field between the positively biased screen grid and negatively biased acceleration grid extracts the propellant ions from the discharge chamber and focuses them through the optics apertures. A fraction of the un-ionized neutrals can also escape through the optics apertures. The propellant ions flow with a kinetic energy corresponding to the acceleration voltage (about 1000eV for the NSTAR thruster, which corresponds to an exhaust speed of about 35 km/s for xenon ions). The escaped neutrals flow at a thermal speed corresponding to the thruster wall temperature (about 0.04eV if chamber wall temperature is at 500K, which corresponds to a speed of about 0.2 km/s for xenon atoms). Charge-exchange collisions will occur between the fast moving propellant ions and the slow moving neutrals, generating slow moving charge-exchange ions and fast moving neutrals. Attracted by the negative voltage of the accelerator grid, those low energy charge-exchange ions generated within the aperture holes and near the grids will impinge upon the grid surface. Such impingement will result in the gradual sputtering of the accelerator grid material, eventually leading to structural failure of the grid. It is well known that ion engine life is primarily limited by grid erosion.

Table 1 lists the nominal geometric and operating conditions for the NSTAR ion optics. The characteristic ion optics dimensions are on the order of O(10^{-3})m. The dominant collision process inside ion optics is charge-exchange collision. The mean-free-path for charge-exchange collisions under the condition inside ion optics is larger than O(1)-O(10)m. Hence, the ion flow inside ion optics is collisionless.

Ion Thruster Plume

The exhaust plume from ion thruster is composed of propellant efflux (propellant beam ions and un-ionized neutrals emitted by the ion optics, and electrons emitted by the neutralizer), nonpropellant efflux (materials sputtered off from ion optics and the neutralizer), and a low-energy charge-exchange plasma generated by collisions between the beam ions and the neutrals within the plume. The sputtered grid material is ejected as neutral atoms in the general direction of the plume. A fraction of the sputtered particles will also become ionized due to charge-exchange collisions with the propellant ions or electron impact ionization. It is well known that both the propellant charge-exchange ions and the ionized sputtered particles can be pushed out of the plume by the electric field in the plume and backflow to interact with the spacecraft.

Fig.3 illustrates plume-spacecraft interactions. The propellant charge-exchange ion is the dominant backflow species. Charge exchange ions can affect spacecraft charging by interacting with the solar arrays and any exposed conducting surface. These ions can also affect space plasma measurements performed on-board by interacting with the ambient plasma and by dominating the local plasma environment surrounding the spacecraft. The xenon charge-exchange ions do not directly contaminate spacecraft surfaces because xenon is not a contaminating species. Spacecraft contamination is caused by the backflow of sputtered grid material, which in the case of DS1 is molybdenum. Deposition of molybdenum particles on spacecraft surface can significantly change the thermo-optical (solar absorptance and emittance) properties of thermal control materials. However, the charge-exchange plasma can play an important role in the backflow of contaminating species through its effects on the electric field and plasma sheath surrounding spacecraft, which in turn controls the trajectories of any ionized particles near the spacecraft. Effects from charge exchange plasma interactions are especially important for interplanetary spacecraft. The number density of the solar wind plasma is only about $1cm^{-3}$ to $10cm^{-3}$. Therefore, the environment surrounding spacecraft will be dominated by the charge-exchange plasma from the thruster plume.

Typical spacecraft dimensions are about O(1)m, while the mean-free-path for charge-exchange ions surrounding spacecraft is larger than O(10)m. Hence, the flow of charge-exchange ions near the spacecraft can be considered as collisionless.

Modeling Approach

The physical processes inside ion optics and in the region surrounding spacecraft have the following common characteristics: there are strong interactions between the space charge carried by the plasma flow and the local electric filed; the ion flow of interest is essentially collisionless; and any electromagnetic wave effects are negligible in this small region. Hence, both ion optics plasma flow and the near-spacecraft plume can be characterized as an electrostatic, rarefied, space charge flow. Computer particle simulation provides the best modeling approach for such a problem.

A model for ion optics or ion thruster plume can be developed using electrostatic particle-in-cell (PIC) [1], which models a plasma as many macro particles and solves particle trajectories, space charge, and the electric field self-consistently. The governing equations are the Poisson's equation

$$\bigtriangledown^2\Phi = -4\pi[n_i - n_e] \tag{1}$$

and Newtown's second law applied to macro-particles

$$\frac{dm\vec{V}}{dt} = q\vec{E}, \;\; \frac{d\vec{x}}{dt} = \vec{V} \tag{2}$$

Such an approach has been used in many recent studies on ion optics modeling and ion thruster plume modeling (see, for example, [2, 3, 4, 5, 6, 9, 10, 11] and references therein). This paper utilizes more generalized, fully 3-dimensional models that we developed recently [13, 14, 15]. The readers are referred to *Wang et al.*[13, 14, 15] for detailed discussions of these models.

MODELING ION OPTICS

The simulation model by *Wang et al.*[14, 15] is used to model ion optics plasma flow. This model is designed in such a way that not only single aperture but also multiple apertures can be included explicitly in the simulation domain (Fig. 4). No assumptions are made to simplify the upstream and downstream boundary conditions. The upstream sheath and ion beam extraction from the discharge plasma are determined self-consistently in the simulation. The simulation is extended into the region far-downstream of the accelerator grid. The location where beamlets are neutralized and charge-exchange ions start to backflow are resolved in the simulation.

The simulation model includes a set of three PIC codes: an ion beamlet code, a neutral particle code, and a charge-exchange ion code. The propellant ions, charge-exchange ions, and neutrals are treated as macro-particles. As the processes of interest to us occur on the ion plasma time scale, the electrons are modeled as an isothermal fluid. In a simulation, the ion beamlet code is used first to simulate ion beam extraction from the discharge plasma, and the neutral particle code is used to track the flow of un-ionized propellant particles. Once a steady state has been achieved for beam ions and neutral particles, the beam ions and neutrals are frozen, and the charge-exchange ion code is activated. Micro-particles representing charge-exchange ions are generated in the simulation domain according to the volumetric charge-exchange ion production rate calculated from

$$\frac{dn_{cex}}{dt} = n_b(\vec{x})n_n(\vec{x})v_b\sigma_{cex} \tag{3}$$

where the beam ion density $n_b(\vec{x})$ is determined by the ion beamlet code and the neutral density $n_n(\vec{x})$ by the neutral particle code. The charge-exchange ion collision cross section σ_{cex} is based on experimental data by *Pullins et al.*[8].

This code is applied to study ion optics plasma flow for the NSTAR ion thruster. Some typical simulation results are shown in Figs. 5 and 6. This simulation is performed for the nominal NSTAR geometric and operating conditions in Table 1. The simulation domain is shown in the right panel of Fig. 4, which includes two quarter-size apertures. A series of test runs are performed to ensure that the upstream boundary is placed well into the discharge chamber and the downstream boundary is placed well beyond the beamlet neutralization location. In the results presented in here, the number of cells used in the simulation domain is $30 \times 30 \times 400$ with a grid resolution corresponding to the Debye length in the discharge plasma ($\lambda_D \sim 0.0037$cm). The number of macro-particles used in beamlet simulation is about 1.8 million and that used in charge-exchange ion simulation is about 9 million.

Fig. 5 shows the 3-dimensional structure of potential contours. The left panel shows potential contours on the side boundary surfaces, and the right panel shows contours on several x-y-cutting planes along the beam direction. Effects from the grid surface potential and the space charge of the beamlet are apparent in the potential contours. Fig. 6 shows ion velocity direction vectors (normalized by velocity magnitude). The propellant ions are extracted from the upstream discharge plasma to form beamlets through the apertures. The beamlets eventually become mixed and neutralized in the far-downstream region. The charge-exchange ions born downstream of the accelerator grid, on the other hand, will backflow toward the accelerator grid. By tracking those ions that impinge upon the grid, we obtain the distributions of

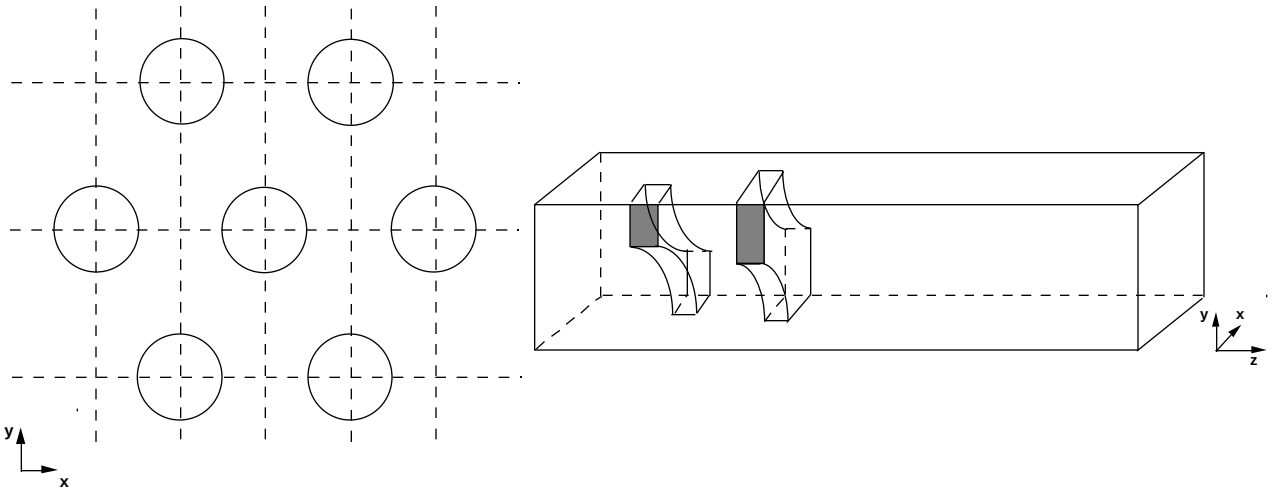

Fig. 4: Simulation domain for ion optics. Left: cross section of a simulation domain with multiple apertures. Right: a simulation domain with two quarter-size apertures.

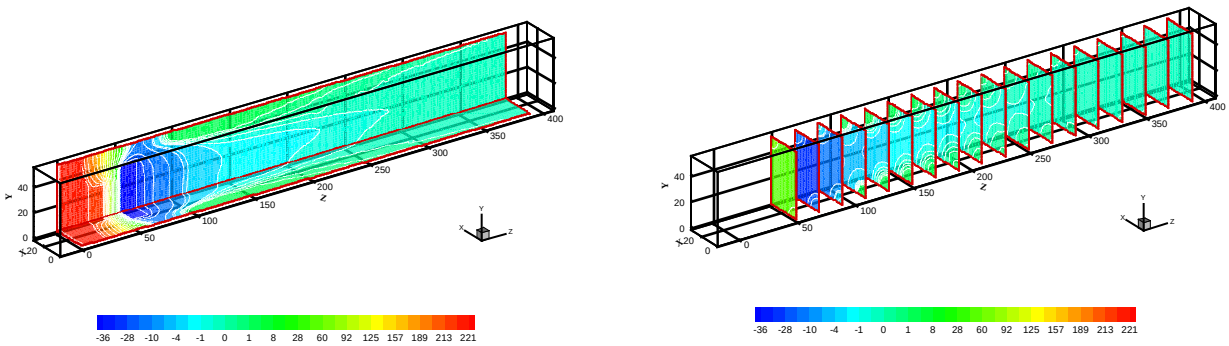

Fig. 5: Potential contours inside ion optics

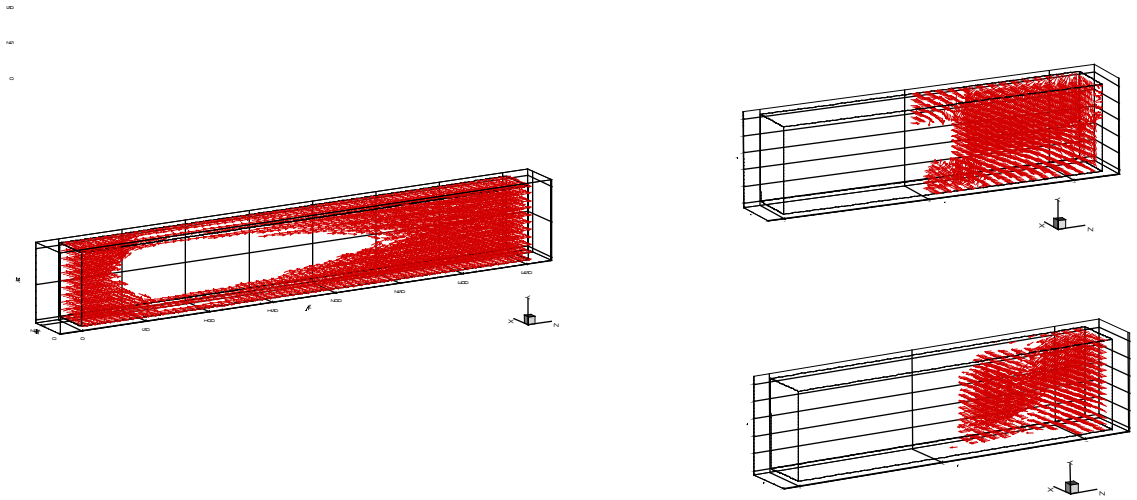

Fig. 6: Ion velocity direction vectors. Left: beam ions. Upper Right: charge-exchange ions originated in the near-downstream region, Bottom Right: charge-exchange ions originated in the far-downstream region.

TABLE 2. Charge-exchange plasma environment at IDS: comparison of in-flight measurement and simulation result

	J_{cex} A/cm^2	n_{cex} cm^{-3}
IDS data	0.9×10^{-7} to 3.3×10^{-7}	1.2×10^6 to 4.4×10^6
Simulation	1.49×10^{-7}	1.43×10^6

impingement current density, incident energy, and incident angle on grid surface. Such information allows us to calculate the depth of erosion on the grid surface due to charge-exchange ion impingement.

During the long duration test of the NSTAR ion thruster, both laser profilometer measurements and post-test destructive examinations were performed to measure accel grid erosion [7]. These grid erosion measurements provide experimental data to validate the simulation model. In Fig. 7, we compare the measured erosion pattern and erosion depth on the downstream face of the accelerator grid with simulation results. The left panel compares a photo of grid erosion pattern on the downstream surface of the accel grid after 8200 hours of operation with the calculated erosion pattern for the same operating condition. The comparison shows that the simulation resolves all of the detailed features shown in the measured erosion pattern. The right panel compares erosion depth along the groove. The maximum eroded depth from simulation is about 208 microns, while the pit depth from the long duration test is 220-230 micron. The comparisons show that the simulation not only accurately predicts the erosion pattern but also gives excellent quantitative agreement with erosion measurements.

MODELING ION THRUSTER PLUME

The simulation model by *Wang et al.*[13] is used to study ion thruster plume in the near-spacecraft region for the DS1 spacecraft. The simulation setup is shown in Fig. 8. We model the DS1 spacecraft as a hexagonal cylinder and the solar array as a thin plate. In this problem, the electric field only affects the dynamics of low energy charge-exchange ions. The propellant beam ions follow a ballistic trajectory due to their much higher kinetic energy compared to the plume potential. The neutral flow is essentially a free molecular flow due to the low collision frequencies. Hence, only the charge-exchange ions are modeled as macro-particles whereas the density distribution of the propellant beam ions and neutrals are modeled analytically. Similar to the ion optics model described in section 3, the electrons are modeled as an isothermal fluid. Macro-particles representing charge-exchange ions are generated at each time step according to the volumetric production rate. These macro-particles are assumed to initially follow a Maxwellian velocity distribution with a temperature corresponding to that of the un-ionized neutral propellant (0.04eV).

A typical simulation result is shown in Fig. 9. For this simulation, the number of cells used is $43 \times 43 \times 71$ with a grid resolution corresponding to the Debye length of the charge-exchange plasma near the thruster exit ($\lambda_D \sim 6$cm). The number of macro-particles used is about 5 million at steady state. Fig. 9 shows the 3-D electric potential contours surrounding DS1 during ion thruster operation. As the electrons are much more mobile than ions, the beam center has a higher electric potential with respect to the edge. Since the ion beam is quasineutral and the beam ion energy is much larger than the potential from the spacecraft, the beam ions are not influenced by the electric field in the plume. In contrast to the beam ions, the low energy charge-exchange ions will be pushed radially outward from the beam region by the electric field in the plume. Once outside the beam region, the charge-exchange ions start to undergo an expansion process which is somewhat similar to the Prandtl-Meyer expansion related to supersonic gas flow over a convex corner [13]. This expansion servers as a presheath which turns the trajectories of the outflowing charge-exchange ions into the upstream direction until they enter into the sheath of spacecraft. The effects from charge-exchange ion outflow and expansion on the electric potential structure are evident in Fig. 9.

The DS1 spacecraft carries an integrated, comprehensive set of diagnostics, ion propulsion diagnostic subsystem (IDS). IDS is designed to characterize ion propulsion induced environments [12]. IDS is located about 75cm from the thruster centerline on the thruster exit plane. In-flight measurements from IDS provide experimental data to validate the simulation model. A comparison of simulation results and measurements is shown for charge-exchange ion current density and number density in Table 2. The measured charge-exchange ion current density J_{cex} and number density n_{cex} are derived from retarding potential analyzer data and Langmuir probe data [12]. The measurements shown in Table 2 was obtained on January 22, 1999 for an ion engine operating condition of ML 83. Ion engine operating parameters provide the input to the simulation model. Compared to IDS measurements, the computed J_{cex} is a factor of 1.7 of the lower bound measurement and a factor of 0.45 of the upper bound measurement. The computed n_{cex} is a factor of 1.2 of the lower bound and a factor of 0.33 of the upper bound.

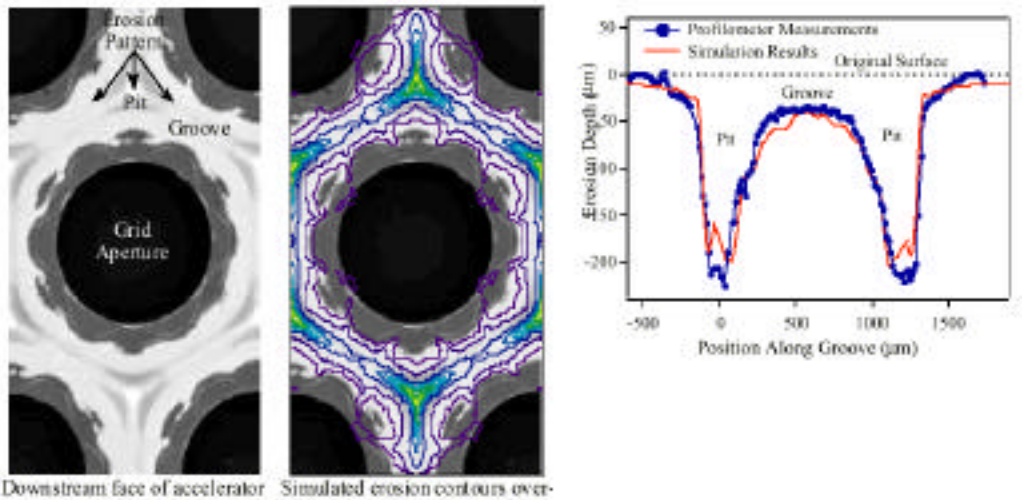

Fig. 7: Comparison of ion optics simulation results and grid erosion measurements

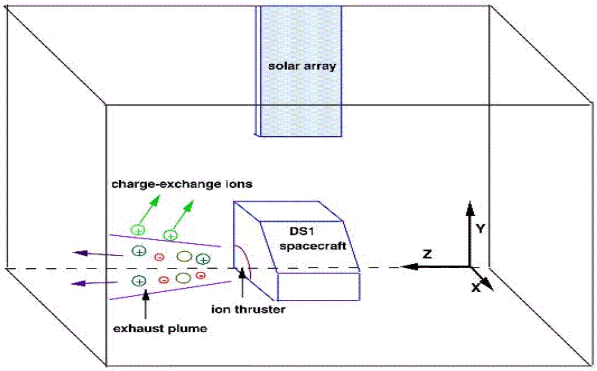

Fig. 8: Model set up for ion thruster plume simulation

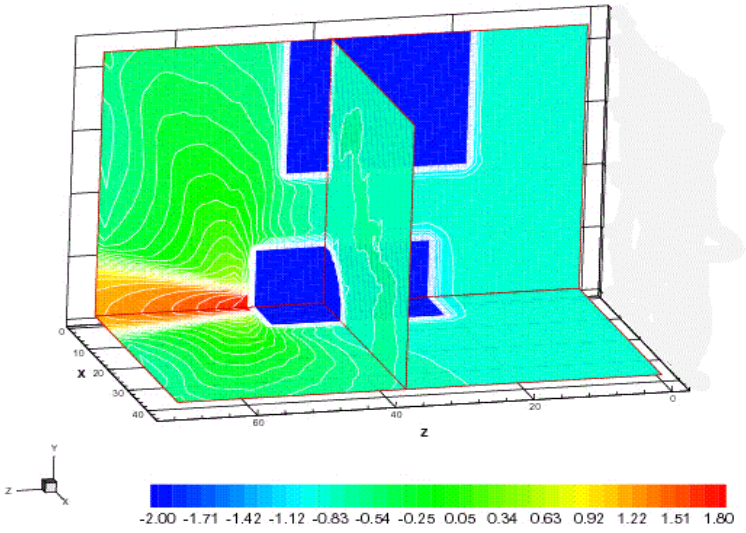

Fig. 9: Electric potential contours surrounding Deep Space 1 during ion thruster operation

SUMMARY AND CONCLUSIONS

This paper discusses two ion thruster modeling studies related to ion thruster design and integration with spacecraft, respectively. In the first study, a fully 3-dimensional particle simulation model of ion optics was developed. This model allows multiple apertures to be included explicitly in the simulation domain, and determines the upstream sheath and downstream beam neutralization through simulations. Simulations are performed for the NSTAR ion thruster optics and results are compared with grid erosion measurements obtained during NSTAR long duration test. It is shown that the simulation not only resolves accurately all the features in the measured erosion pattern but also gives excellent quantitative agreement with measured erosion depth. In the second study, a fully three-dimensional particle simulation model of ion thruster plume was developed. This model computes the thruster induced environment over the entire downstream-to-upstream region surrounding a spacecraft. Simulations are performed for the Deep Space 1 spacecraft and results are compared with in-flight measurements of charge-exchange plasma obtained by the IDS instruments on DS1. Again, the results show good agreement. The results of these two studies also suggest that first-principle based modeling may be used as engineering design tools for ion thrusters under current high-performance computing capabilities.

ACKNOWLEDGMENTS

This research is supported by NASA New Millennium Deep Space 1 mission and NASA Solar Electric Propulsion Technology Application Readiness Project. Simulations are performed on the Cray SV1-1A supercomputer at JPL with funding from NASA Offices of Space Science, Mission to Planet Earth, and Aeronautics.

REFERENCES

1. Birdsall,C. and Langdon,A., *Plasma Physics via Computer Simulation*, McGraw-Hill, New York, 1985.
2. Boyd,I., et al., Monte Carlo simulation of neutral xenon flows in electric propulsion devices, *J. Propulsion and Power*, 14(6), pp1009 (1998).
3. Muravlev,Y. and Shagayda,A., Numerical modeling of extraction systems in ion thrusters, *IEPC-99-162* (1999).
4. Nakano,M., and Arakawa,Y., Ion thruster lifetime estimation and modeling using computer simulation, *IEPC-99-145* (1999).
5. Nakayama,Y., and Wilbur,P., Numerical simulation of ion beam optics for many-grid systems, *AIAA-2001-3782* (2001).
6. Peng,X., et al., Particle simulation of ion optics and grid erosion for two-grid and three-grid systems, *Rev. Sci. Instrum.*, 65(5), pp1770 (1994).
7. Polk,J., et al., An overview of the results from an 8200 hour wear test of the NSTAR ion thruster, *AIAA 99-2446* (1999).
8. Pullins,S., et al., Ion dynamics in Hall effect and ion thrusters: $Xe^{+}+Xe$ symmetric charge transfer, *AIAA 2000-0603* (2000).
9. Samanta Roy,R., et al., Ion-thruster Modeling for Backflow Contamination, *J. Spacecraft and Rockets*, 33(4), pp525 (1996).
10. Tartz,M., et al., Validation of a grid-erosion simulation by short-time erosion measurements, *IEPC-99-147* (1999).
11. VanGilder,D., et al., Hybrid Monte Carlo Particle-in-Cell Simulation of an Ion Thruster Plume, *J. Propulsion and Power*, 15(4), pp530 (1999).
12. Wang,J., et al., Deep Space 1 investigations of ion propulsion plasma environment, *J. Spacecraft and Rockets*, 37(5), pp545 (2000).
13. Wang,J., et al., Three-dimensional particle simulation modeling of ion propulsion plasma environment for Deep Space 1, *J. Spacecraft and Rockets*, 38(3), pp433 (2001).
14. Wang,J., et al., 3-D particle simulations of NSTAR ion optics, *IEPC-01-085* (2001).
15. Wang,J., et al., Three-dimensional particle simulation modeling of ion optics plasma flow and grid erosion, submitted to *J. Propulsion and Power* (2002).